

ON-OFFSHORE SEDIMENT TRANSPORT RATE  
IN THE SURF ZONE

Toru Sawaragi

Professor of Civil Engineering  
Osaka University, Osaka, Japan

and

Ichiro Deguchi

Research Associate of Civil Engineering  
Osaka University, Osaka, Japan

ABSTRACT

In this paper, models of the distribution of net on-offshore sediment transport based on two-dimensional equilibrium beach profiles and an equation of continuity of sediment transport are proposed. Various parameters of net on-offshore sediment transport in those models are discussed. Further, the relative importance of bed load and suspended load in the two-dimensional beach deformation are examined by measuring both of them on model beach experiments.

1. Introduction

A problem of fundamental importance to the mechanics of sediment transport on beaches under wave and wave-induced current system is the relative magnitude of the littoral sand drift and on-offshore sediment transport. In the previous report (Sawaragi et al., 1978), the authors have formulated the littoral sediment transport rate considering long-shore current as a sediment transporting flow. However, as to on-offshore sediment transport rate, the authors could not evaluate quantitatively because of the complexity of mechanics of sediment transport.

The purpose of this study is to examine the relation between on-offshore sediment transport and the deformation process of two-dimensional beach profile. The first half of this paper will be constructed around a model of the distribution of net on-offshore sediment transport rate based on experimental results about two-dimensional beach deformation which were conducted by many investigators. The final part of this paper will examine a relative importance of suspended and bed load in the two-dimensional beach deformation by measuring directly suspended and bed loads in two-dimensional model beach experiments.

2. Model of the distribution of net on-offshore sediment transport rate along a beach profile

As suggested by Tanaka et al. (1973) and Horikawa et al. (1974), beach profiles which seem to reach a quasi-equilibrium condition can be classified into three types as shown in Fig. 1. The distribution of net

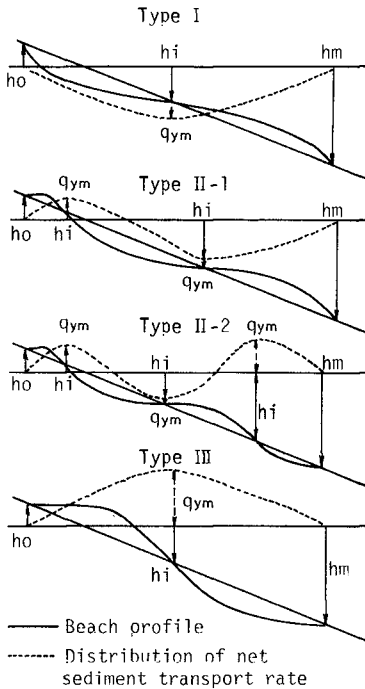


Fig.1 Model of the distribution of net on-offshore sediment transport rate

on-offshore sediment transport, which would have taken place in the processes of those beach deformation, can be modelled as dotted lines in Fig.1 from the equation of continuity of sediment transport. In Type I (erosion type), the direction of net on-offshore sediment transport is always toward offshore. In Type III (accretion type), onshore net sediment transport takes place in the entire range of beach profile. In Types II-1 and II-2, both onshore and offshore net sediment transport spring up.

The distribution of net on-offshore sediment transport rate can roughly be determined by  $h_0, h_m, h_i$  and  $q_{ym}$  shown in Fig.1 where,  $h_0$  and  $h_m$ : the critical height and depth of beach deformation, respectively,  $h_i$ : the depth of the point of intersection of two beach profiles measured in succession, i.e., the depth where the maximum net on-offshore sediment transport takes place,  $q_{ym}$ : the maximum net on-offshore sediment transport rate, and  $h_0$  is taken upward, while  $h_m$  and  $h_i$  are taken downward from the still water level.

The authors rearranged about 80 experimental results on the two-dimensional beach deformation conducted by many investigators and evaluated  $h_0, h_m, h_i$  from the beach change of beach configurations by

profiles, and calculated  $q_{ym}$  from the using the equation of continuity of sediment transport. In the following sections, these four characteristic quantities are analyzed by taking account of previous results obtained from the two-dimensional model beach experiments.

3. Analysis of  $h_0, h_m, h_i$  and  $q_{ym}$  which determine the distribution of net on-offshore sediment transport rate.

The four characteristic quantities will be expressed by the fluid density  $\rho$ , fluid kinematic viscosity  $\nu$ , density of sediment  $\rho_s$ , median grain size  $d_{50}$ , wave height  $H$ , wave period  $T$ , beach slope  $i$ , gravity acceleration  $g$ , friction velocity  $u_*$ , wave running time  $t_s$ , and so on. Some important parameters such as the Shield's parameter

$u_*^2/(\rho_s/\rho-1)gd_{50}$  and the surf similarity parameter  $\xi=i/\sqrt{H_0/L_0}$  are already derived by combining above-cited variables to explain various phenomena in the surf zone. So far, however, there is no objective way to judge whether the beach profile reaches equilibrium or not. The authors, first, examine the time variations of  $h_o, h_m, h_i$  and  $q_{ym}$  to determine the wave running time for quasi-equilibrium beach profile.

3-1 Time-variations of the characteristic variables

Time-variations of  $h_o, h_m, h_i$  and  $q_{ym}$  of typical 2 cases in Type I and Type III are shown in Figs.2 and 3, respectively. In the figures,  $q_{ym}$  are calculated from differences of the water depth  $\Delta h$ , measured in succession with time interval  $\Delta t$ , by using the equation of continuity of the sediment transport. Therefore, they are given as average values taken over the time interval  $\Delta t$ . From Figs.2 and 3, the following results can be pointed out.

- 1) Net offshore sediment transport does not readily decrease even after a fairly long running time as seen in Fig.2. While, onshore net sediment transport decays soon, as seen in Fig.3.
- 2) In accordance with 1),  $h_o$  and  $h_m$  in Type I and  $h_m$  in Type II-1 increase after a large number of waves propagated. On the other hand,  $h_o$  and  $h_m$

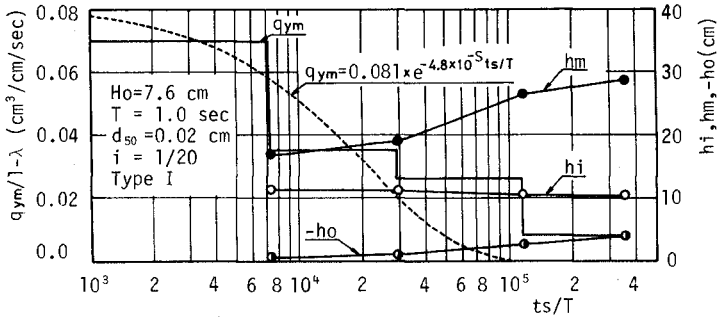


Fig.2 Time-variations of characteristic quantities of Type I

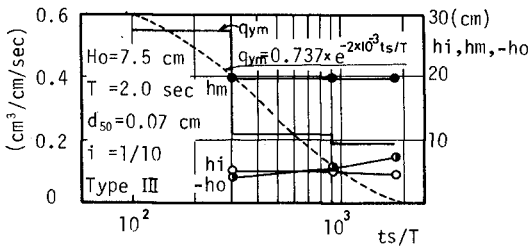


Fig.3 Time-variations of characteristic quantities of Type III

in Type III and Type II-2 almost remain constant or increase a little with increasing the running time.

3)  $h_i$  does not indicate significant changes with time.

Taking these results into account, beach profiles after  $7.2 \times 10^4$  waves propagated were picked up to analyze  $h_o$ ,  $h_m$  and  $h_i$ . In the case where the beach profile at this running time was not measured, we estimated those quantities by interpolating from the time-variations of them. The data, whose running time were less than  $7.2 \times 10^4 T$ , were omitted. However, experimental results of Saville (1957) who employed waves almost corresponding the full scale waves and Rector (1954) which have been quoted by many investigators were analyzed for reference, although they did not satisfy this limitation of running time.

On the other hand, we can assume the time-variations of  $q_{ym}$  expressed as Eq. (1) to clearly grasp the rate of decay of  $q_{ym}$  with running time.

$$q_{ym} = q_{ym0} \exp(-At_s/T) \quad (1)$$

where  $q_{ym0}$  is the initial value of  $q_{ym}$  and  $A$  is a constant. Here,  $q_{ym0}$  and  $A$  are calculated by the following procedure:

- 1) Select the data whose running times are more than  $7.2 \times 10^4 T$  in which beach profiles were measured at least 3 times.
- 2) Let  $t_s = 0, t_{s1}, t_{s2}, \dots$  be the times when the beach profile was measured and  $q_{ym1}, q_{ym2}, \dots$  be the maximum on-offshore sediment transport rate in the time interval  $\Delta t_1 = t_{s1}, \Delta t_2 = t_{s2} - t_{s1}, \dots$
- 3) Calculate  $q_{ym0}$  and  $A$  by substituting  $q_{ym} = q_{ym1}$  at  $t_s = t_{s1}/2$  and  $q_{ym} = q_{ym2}$  at  $t_s = (t_{s1} + t_{s2})/2$ .

In Figs. 2 and 3, Eq. (1) determined by the above-mentioned procedure are also shown by dotted curves. As can be seen from these figures, it is found that the time-variation of  $q_{ym}$  can be expressed fairly well by Eq. (1) and at  $t_s/T = 7.2 \times 10^4$ , the maximum onshore net sediment transport rate  $q_{ym}$  in Types III and II-2 almost diminish and the maximum offshore net sediment transport rate of Types I and II-1 become less than 25% of their initial value  $q_{ym0}$ .

### 3-2 Analysis of $h_o$

$h_o$  will be determined by factors which control a wave run-up height and a change of shore line. The wave run-up height is said to be closely related to the surf similarity parameter  $\xi$  (Battjes, 1974). While, the change of shore line should be considered as one part of the whole beach deformation rather than related to local parameters near the shore line. Hence, the authors use the non-dimensional force,  $N_s = H_o/T \sqrt{(\rho_s/\rho - 1)gd_{s0}}$  as the parameter to indicate the magnitude of the ability of the beach to deform. The derivation of  $N_s$  will be mentioned latter. Fig. 4 shows the relation between  $h_i/H_o$  and  $\xi$  with  $N_s$  as a parameter. From this figure, it is found that  $h_i/H_o$  increases with increasing  $\xi$  and that for the same value of  $\xi$ ,  $h_i/H_o$  also increases with increasing  $N_s$ .

### 3-3 Analysis of $h_m$

In the initial stage of the beach deformation,  $h_m$  can not be deeper than the critical depth for an initial sediment movement. Generally,

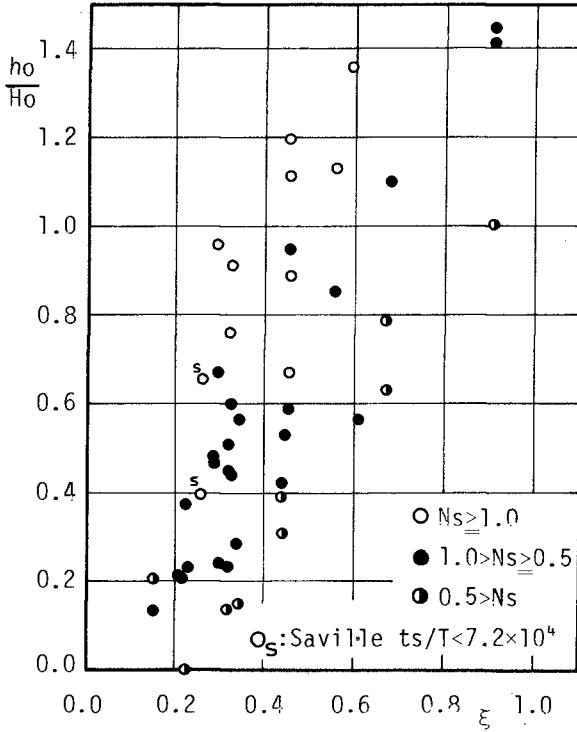


Fig.4 Relation between  $h_o/H_o$  and  $\xi$

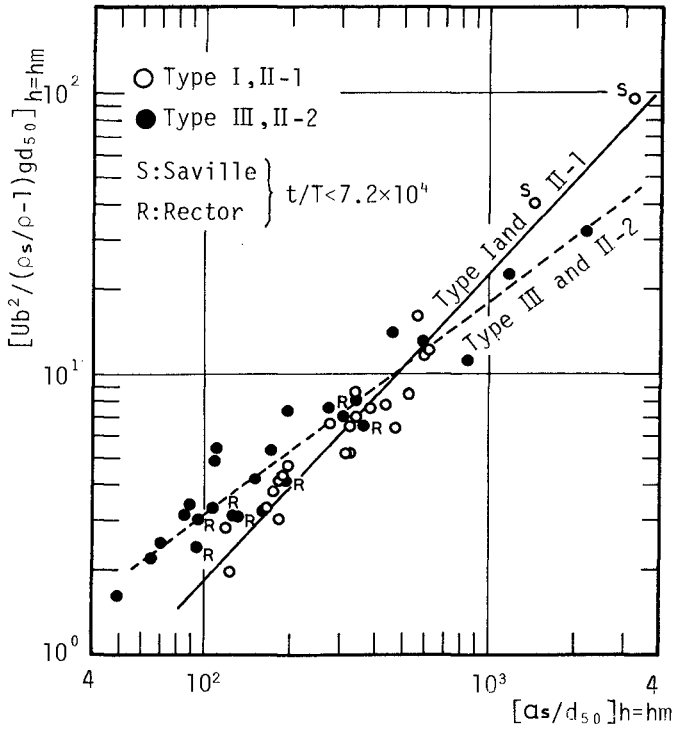


Fig.5 Relation between  $U_b^2 / (\rho_s / \rho - 1) g d_{50}$  and  $a_s / d_{50}$  at  $h=hm$

the critical depth for the sediment movement is determined from the balance between the forces acting on a grain and the resistance force of the grain which can be given as follow:

$$(\pi/6)gd_{50}(\rho_s-\rho)\tan\phi = K(\pi/4)d_{50}^2\rho f u_b^2 \quad (2)$$

where  $\tan\phi$  is the friction angle of the sediment,  $f$  the friction factor,  $u_b$  the maximum water particle velocity at the bottom, and  $K$  the coefficient.  $f$  is usually expressed by  $u_b\delta/\nu$  or  $u_b^2 T/\nu$  in a laminar region and  $a_s/Z_0$  in a turbulent region where  $\delta=(\nu T/2\pi)^{1/2}$ ,  $a_s=Tu_b/\pi$  and  $Z_0$  the equivalent roughness height. However, the effect of Reynold's number on the initial movement of sediment seems to be small compared with  $a_s/Z_0$  (Dingler,1975). Hence, Eq.(2) can be given as follow:

$$u_b^2/(\rho_s/\rho-1)gd_{50}\approx 1/f\approx F(a_s/Z_0) \quad (3)$$

Assuming that the same relation as Eq.(3) holds with  $h_m$ , the authors calculated  $u_b^2/(\rho_s/\rho-1)gd_{50}$  and  $a_s/Z_0$  at  $h=h_m$  by using the linear wave theory. The results are shown in Fig.5. In this calculation,  $Z_0$  is taken equal to  $d_{50}$  in order to take account of only the skin friction regardless of the bottom configuration according to Madsen(1976). As seen from Fig.5, the relation between  $u_b^2/(\rho_s/\rho-1)gd_{50}$  and  $a_s/d_{50}$  at  $h=h_m$  can be approximated fairly well by the following equations:

$$u_b^2/(\rho_s/\rho-1)gd_{50} = B(a_s/d_{50})^n \quad (4)$$

in which,

$$\begin{aligned} B &= 0.18 & n &= 1.1 & \text{for Type I and Type II-1} \\ B &= 0.10 & n &= 0.75 & \text{for Type III and Type II-2} \end{aligned} \quad (5)$$

By using the linear wave theory and  $N_s = H_0/T/\sqrt{(\rho_s/\rho-1)gd_{50}}$ , Eq.(4) can be modified as Eqs.(6) and (7).

$$\{(H/H_0)(1/\sinh kh_m)\}^{-1} = CN_s(d_{50}/L_0)^m \quad (6)$$

$$\begin{aligned} C &= 400 & m &= 0.6 & \text{for Type I and Type II-1} \\ C &= 20 & m &= 0.3 & \text{for Type III and Type II-2} \end{aligned} \quad (7)$$

The left hand side of Eq.(6) is the function of  $h_m/L$  only. And if  $N_s$  and  $d_{50}/L_0$  are given,  $h_m/L$  can be calculated from Eqs.(6) and (7). Fig.6 shows the comparison of  $h_m$  calculated from Eq.(6) with  $h_m$  measured from the beach profile. From this figure, it is found that Eq.(6) together with Eq.(7) give a sufficiently accurate estimate of  $h_m$ .

### 3-4 Analysis of $h_i$

$h_i$  is defined as the depth where the maximum on-offshore sediment transport takes place. The limit depth of "D-profile" proposed by Swart(1970), "cut-depth" defined by Hallermeier(1977) seem to correspond to  $h_i$  of Types I and II-1. "Stable point" proposed by Raman et al. (1972) may also equivalent to  $h_i$ . Although the concept of "D-profile" or "cut-depth" can be applied only to the beach of Types I and II-1,  $h_i$  as defined above, can be applied extensively to all types of beach profiles.

In the consideration of  $h_i$ , it is necessary to take into account the difference of the mode of sediment transport between Type I and Type III. The causes of net on-offshore sediment transport have been studied for long time and may be summarized as follows:

- 1) stational flow such as mass transport current due to waves.
- 2) asymmetry of water surface profile, ie, asymmetry of the time-vari-

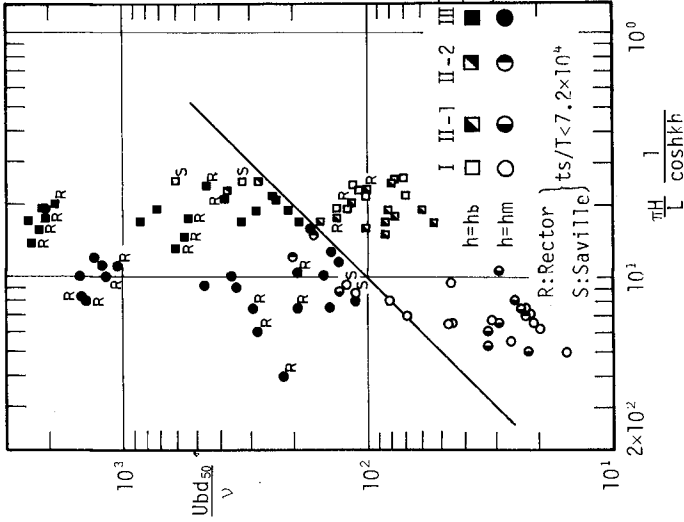


Fig. 7 Relation between  $Ubd_{50}/v$  and  $(\pi H/L)(1/\cosh kh)$  at  $h=hb$  and  $h=hm$

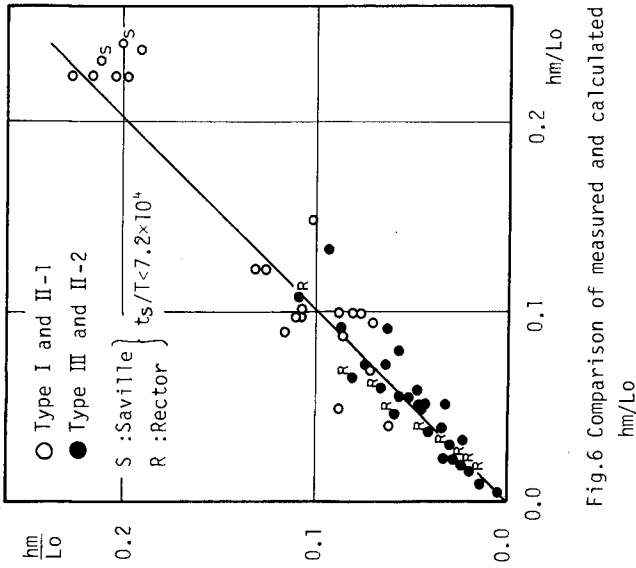


Fig. 6 Comparison of measured and calculated  $hm/Lo$

ation of water-particle velocity.

3) effect of gravity, i.e., the existence of beach slope.

4) distorted profile of time-variation of the concentration of suspended sediment due to asymmetrical sand ripple or breaking waves.

Referring from theoretical and experimental results by Sato et al. (1962), Inman et al. (1963), Horikawa et al. (1974) and Bowen (1979), the necessary condition for the occurrence of net offshore sediment transport seems to be the existence of sufficient amount of suspended sediment, and net onshore sediment transport is mainly caused by bed load.

However, in the surf zone, although the asymmetrical property of time-variations of water-particle velocity increases, ripples usually disappear and the existence of the steady flow becomes dubious because of large turbulence brought by breaking waves. Hence, so far, the authors can not explain the reason why net onshore sediment transport can take place in the entire beach profile of Type III and net offshore sediment transport happens in the whole beach of Type I. Then, to begin with, the authors examine the direction of net on-offshore sediment transport in the offshore regions of three types of beach profiles by using two parameters proposed by Sato et al. (1962). They give the criteria for the occurrence of net on-offshore sediment transport on a horizontal bed by a function of sediment Reynold's number  $u_b d_{50} / \nu$  and the amplitude of non-dimensional pressure gradient at the bottom by waves  $(-1/\rho g)(\partial p/\partial x) = (H/L)(\pi/\cosh kh)$ . They also found that asymmetrical ripples caused net offshore sediment transport by using radio active tracers. Although  $u_b d_{50} / \nu$  is a non-dimensional parameter, it expresses a magnitude of drag force acting on a grain in a fluid and  $(-1/\rho g)(\partial p/\partial x)$  indicates the relative magnitude of the acceleration of water-particle to that of the gravity. Fig. 7 shows the relation between  $u_b d_{50} / \nu$  and  $(H/L)(\pi/\cosh kh)$  at  $h=h_b$ , calculated from the new-breaker-index presented by Goda (1970), and  $h=h_m$ . Again,  $u_b$  and  $L$  were calculated by the small amplitude theory. Taking into account the direction of net on-offshore sediment transport of Type I and Type III, the direction of net on-offshore sediment transport can be distinguished by Eq. (8)

$$u_b d_{50} / \nu \begin{cases} < (H/L)(\pi/\cosh kh) \times 10^3 & \dots \text{ offshore} \\ > & \dots \text{ onshore} \end{cases} \quad (8)$$

Taking the ratio of  $u_b d_{50} / \nu$  to  $(H/L)(\pi/\cosh kh)$  and let the ratio be  $N_{sr}$ , the criteria of Eq. (8) can be written in a simple form,

$$N_{sr} = (u_b d_{50} / \nu) / \{(H/L)(\pi/\cosh kh)\} = g T d_{50} / 2 \pi \nu$$

$$N_{sr} \begin{cases} < 10^3 & \dots \text{ offshore} \\ > & \dots \text{ onshore} \end{cases} \quad (9)$$

However, as can be seen from Fig. 7, two data of Saville (1957) can not be classified by Eq. (8). He employed large waves as in the field and  $H_o/L_o$  of his experiments were larger than other cases. Therefore, to apply Eq. (8) or Eq. (9) to the large scale model beach as the field, some modifications including the effect of wave height itself or  $H_o/L_o$  explicitly seems to be required.

The direction of net sediment transport in Types II-1 and II-2 are also shown in Fig. 7, and they are classified by Eq. (9). This means that the change of the direction of net on-offshore sediment transport in

in these two types will occur in the surf zone.

As discussed above, the direction of net sediment transport in the offshore region can be determined by  $N_{sr}$ . On the other hand,  $h_i$  seems to be closely related to wave breaking as the first order action of fluid motion. So, the authors examine the relative depth of  $h_i$  to  $h_b$ ,  $h_i/h_b$  of three types of beach profiles. Fig.8 shows the relation between  $h_i/h_b$  and  $N_{sr}$ . It can be seen from this figure that for the offshore net sediment transport of Types I and II-1,  $h_i/h_b$  ranges between  $1.0 < h_i/h_b < 1.5$ , for the onshore net sediment transport of Type III,  $0.3 < h_i/h_b < 0.9$  and for the onshore net sediment transport of Type II-1,  $-0.4 < h_i/h_b < 0.0$ . This indicates that a longshore bar in a storm beach (Type I or Type II-1) has to be generated in the offshore region. For the beach of Type II-2, no significant tendency can be found out for the deficiency of the data.

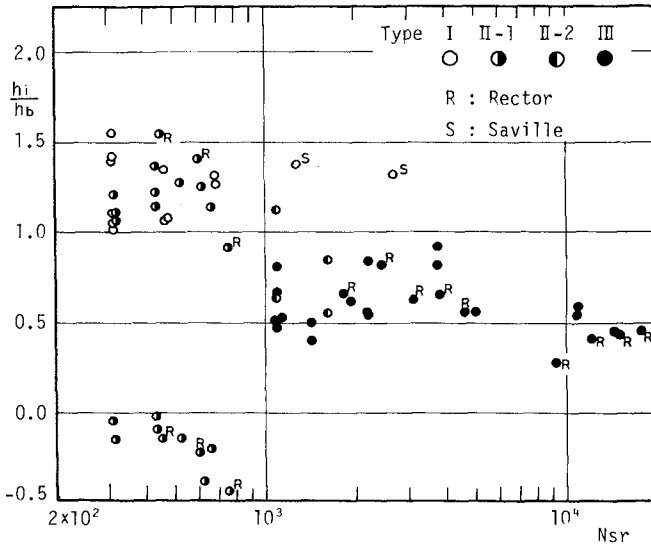


Fig.8 Relation between  $h_i/h_b$  and  $N_{sr}$

Because  $h_i$  of Types I and II-1 appears outside the surf zone, the procedure proposed by Hallermeier(1977) seems to be effective. Hence, the authors compared  $h_s$  calculated according to Hallermeier with  $h_i$  measured from the beach profile of Types I and II-1. As a result, the correlation between  $h_i$  and  $h_s$  is relatively high for small scale experiments, however,  $h_s$  seems to give smaller values of  $h_i$  for large-scale experiments. On the other hand, within the breaker zone, wave characteristics and wave-induced flow pattern are controlled by  $H_0/L_0$  and  $\bar{i}$

(Nakamura et al., 1966). Hence,  $h_i$  for onshore net sediment transport of Type III may also be controlled by  $H_o/L_o$  and  $i$ . The authors also discussed the relation between  $h_i$  of Type III and those two parameters. It is found that  $h_i/h_b$  have a tendency to decrease with decreasing  $H_o/L_o$ , however,  $i$  seems to have little influence on  $h_i/h_b$ .

### 3-5 Analysis of $q_{ym}$

Referring Madsen's presentation (1976), the time averaged rate of on-offshore sediment transport by bed load  $\bar{q}_y$ , i.e., the amount of sediment which have a capacity to be transported as net on-offshore sediment transport, can be expressed as follow:

$$\bar{q}_y / W_o d_{s0} = D (u_*^2 / (\rho_s / \rho - 1) g d_{s0})^n \quad (10)$$

where  $D$  is a coefficient,  $W_o$  the settling velocity of sediment and  $n=3$ . Assuming that the same kind of relation as Eq. (10) can be applied to suspended load and that the direction and the rate of net sediment movement can be expressed by  $N_{sr}$ ,  $H_o/L_o$  and  $i$ , net on-offshore sediment transport rate  $q_y$  will be given as a first order approximation by

$$q_y / W_o d_{s0} \approx q F_1 (N_{sr}, H_o/L_o, i) \cdot F_2 (t_s/T) \\ = D (u_*^2 / (\rho_s / \rho - 1) g d_{s0})^n \cdot F_1 (N_{sr}, H_o/L_o, i) \cdot F_2 (t_s/T) \quad (11)$$

Further, it seems reasonable to assume the turbulent flow condition near  $h=h_i$  and consequently a constant friction factor. Then, for Types I and II-1,  $u_*$  at  $h=h_i$  ( $> h_b$ ) can be replaced by  $(H_o/T)(H/H_o \sinh kh)_{h=h_i} = (H_o/T)F_3(h_i/L_o)$ , and  $h_i/L_o$  is also expressed by  $H_o/L_o$  according to Hallermeier (1977). Hence, the maximum net sediment transport  $q$  becomes

$$q_{ym} / W_o d_{s0} = q_{ym0} \exp(-At_s/T) \\ = E (H_o/T / \sqrt{(\rho_s / \rho - 1) g d_{s0}})^{2n} F (N_{sr}, H_o/L_o, i) \exp(-At_s/T) \quad (12)$$

where  $N_s = H_o/T / \sqrt{(\rho_s / \rho - 1) g d_{s0}}$  and  $E$  is the coefficient of proportionality.  $N_s$  was already used to analyze  $h_o$  and  $h_m$ . The authors further consider that Eq. (12) can be applied to Types III and II-2.

Fig. 9 shows the relation between  $A$  in Eq. (12) and  $N_s$ . It can be seen that  $A$  is closely related to  $N_s$  and the direction of net on-offshore sediment transport. Namely, the larger, the  $N_s$ , the faster net sediment transport decays. And onshore net sediment transport decreases faster than offshore sediment transport.

Finally, Fig. 10 shows the relation between non-dimensional net on-offshore sediment transport rate  $q_{ym0}^*$  and  $N_s$ . Here,  $q_{ym0}^*$  is derived by taking four parameters in Eq. (12) into account as follow:

$$q_{ym0}^* = (q_{ym0} / W_o d_{s0})^{2n} (1/\lambda) (1/N_{sr}) (H_o/L_o) \quad (13)$$

where  $\lambda$  is the porosity of sand. From Fig. 10, it is concluded that  $q_{ym0}^*$  is proportional to  $N_{sr}$  regardless of the direction of net on-offshore sediment transport. And the exponent  $n$  in Eq. (10) is 3. The result corresponds to that obtained by Madsen et al. (1976).

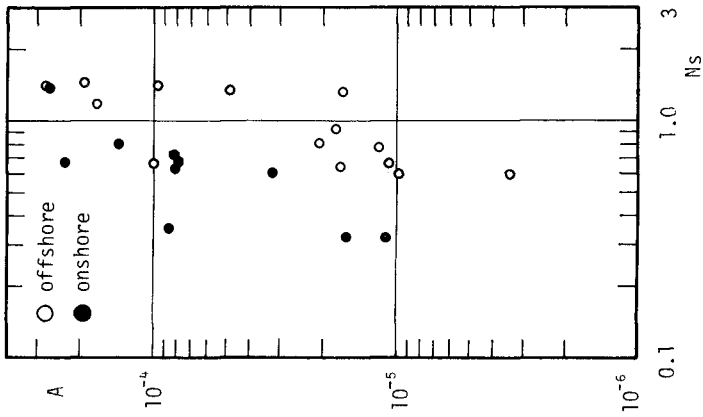


Fig.9 Relation between A and  $N_s$

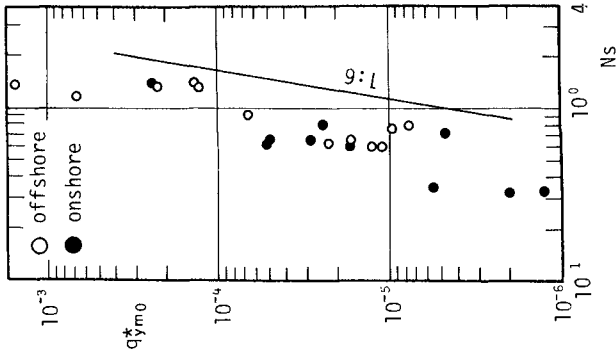


Fig.10 Relation between  $q_{yrmo}^*$  and  $N_s$

#### 4. Experiments to measure on-offshore sediment transport rate in the two-dimensional model beach

Since net on-offshore sediment transport discussed above includes both bed and suspended loads, the relative magnitude of bed load and suspended load can not be examined. In this section, based on the experimental results, relative importance of bed load and suspended load in the deformation of two-dimensional model beach is discussed.

#### 4-1 Equation of continuity of the sediment transport including suspended sediment

Consider the co-ordinate system taken X-axis horizontal to the shore line, positive y-axis shoreward, positive Z-axis vertically upward from the stillwater level. The diffusion equation for any arbitrary volume is

$$\partial C / \partial t = -\nabla \cdot (\vec{C} \vec{V}_s) \quad (14)$$

where  $C$  is the sediment concentration,  $\vec{V}_s$  the sediment-particle velocity vector. After taking time average and integrating Eq.(14) from  $z=-h$  (bottom) to  $Z=\eta$  (free surface), the equation of continuity can be obtained as follow:

$$\frac{\partial}{\partial t} \left( \int_{-h}^{\eta} C \, dz + (1-\lambda)h \right) + \frac{\partial}{\partial x} \int_{-h}^{\eta} q_x \, dz + \frac{\partial}{\partial y} \int_{-h}^{\eta} q_y \, dz = 0, \quad (15)$$

where  $(q_x, q_y) = (u_s C, v_s C)$ ,  $\vec{V}_s = (u_s, v_s, w_s)$ ,  $(1-\lambda)\partial h / \partial t = [w_s C]_{z=-h}$

In the previous section, the authors consider Eq.(11) as a first order approximation of  $q_y = v_s C$ . In Eq.(15),  $z=-h$  corresponds to bed load and  $z>-h$  to suspended load, respectively.

Based on these consideration, the authors examine the relative importance of bed load and suspended load by measuring directly bed load and suspended load in model beach experiments.

#### 4-2 Experimental procedure

Two wave tanks of different dimension were used. One is 26m long, 1.5m wide and 1.8m high, and other one is 51m long, 0.64m wide and 0.97m high. Two kinds of beach materials, i.e.,  $d_{50} = 0.54\text{mm}$ ,  $\rho_s = 2.65\text{gr/cm}^3$  and  $d_{50} = 0.34\text{mm}$ ,  $\rho_s = 2.68\text{gr/cm}^3$  were used to form a model beach of 1/20 initial beach slope. The bed load was measured by a sand trap composed of an outer casing and inner box made of a tin plate. The inner box has two compartments to separately measure the amount of onshore and offshore sediment transport rate. The dimension of this inner box is 10cm in width, 10cm in length and 5cm in depth. While the beach profile was developed, the inner box was not installed and the outer casing was buried into the bottom sand bed. Just before the measurement was conducted, the outer casing was pulled up to the bottom surface and sands in it were taken out to replace them with the inner box. Bed load was measured at 10 different locations covering from swash zone to the offshore zone, and the measured time was from 2 to 6min. The average sediment transport rate  $Q_{bt}$  and net sediment transport rate  $Q_{bnet}$  were calculated from the sum and the difference of the amounts of sediment trapped in both shoreward and seaward compartments respectively in the unit of (dry weight/cm/sec). The suspended load was measured by collecting the water samples through siphons with intake nozzles as shown in Fig.11. the reasons why such a



variation of the velocity of fluid sucked through the intake nozzle which is calculated from the generalized Bernoulli's theorem; pressure equation. A head difference between the intake nozzle and the outlet was adjusted to coincide the intake velocity with the maximum water-particle velocity in both direction of offshore and onshore. However, when the orientation of intake nozzles directed onshore or offshore, a few sediments which were moving in the direction of offshore or onshore, seemed to be sucked. Consequently, the measured concentration might be little larger than the true concentration. Besides, due to an accuracy of weighing dry sands in the sample, the accuracy of concentration measured by this method decreases when  $C$  is less than  $10^4$  ppm.

The authors confirmed the reliability of the siphon by comparing the concentrations measured by the siphon with those of ductivity meter using an optical method.

Table-1 Experimental conditions

## 4-3 Experimental results

6 experiments were conducted. Their detailed conditions are shown in Table-1. In three cases of  $N_{sr}=636$ , suspended load will be expected to dominate and in the other three cases of  $N_{sr}>1200$ , bed load will be predominate.

H cm	T sec	$d_{50}$ mm	$\rho_s/\rho$	$N_{sr}$
17.8	1.2	0.34	2.68	636
7.3	1.2	0.34	2.68	636
3.8	1.2	0.34	2.68	636
33.1	1.7	0.54	2.65	1431
12.4	1.7	0.54	2.65	1431
5.4	1.5	0.54	2.65	1263

i) Time-averaged on-offshore sediment transport by bed load  $Q_{bt}$  and suspended load  $Q_{st}$

First, let's investigate the difference of the relative magnitude of  $Q_{bt}$  and  $Q_{st}$  between two beaches of different  $N_{sr}$ . Fig.12(a) and (b) show two examples of the distributions of  $Q_{bt}$  and  $Q_{st}$ . When  $N_{sr}=636$ , as shown in Fig.12(a), time-averaged suspended load  $Q_{st}$  clearly surpasses bed load  $Q_{bt}$  in amount. The ratio of the maximum time-averaged sediment transport rate  $Q_{st}/Q_{bt}$  is about 2.0. While in the case of  $N_{sr}=1263$ , as shown in Fig.12(b), suspended load is less than bed load and the ratio of the maximum transport rate  $Q_{st}/Q_{bt}$  is 0.5.

The authors also measured a bottom shear stress on a fixed flat bed by a shear meter. Details of the shear meter are described in the previous paper (Sawaragi et al., 1978). From Fig.12 and the results of the measured shear stress, it was found that  $Q_{st}$  was larger than  $Q_{bt}$  in the region of  $U_* / W_0 > 0.8$ , and  $Q_{bt}$  became larger than  $Q_{st}$  when  $U_* / W_0 < 0.8$ . However,  $U_*$  measured on a fixed bed, does not include the effect of the bottom roughness. So, in order to determine the strict criterion for the initiation of sediment suspension, it is necessary to clarify the sediment movements on the bottom which are closely related to the water-particle motion near the bottom.

ii) Relative importance of suspended load versus bed load to the beach deformation

Finally, the authors examine the relative importance of suspended load versus bed load to the beach deformation by investigating the relations among net sediment transport rate  $Q_{net}$  calculated from the time-variations of beach profiles, measured net on-offshore sediment transport rate by suspension  $Q_{snet}$  and bed load  $Q_{bnet}$ .

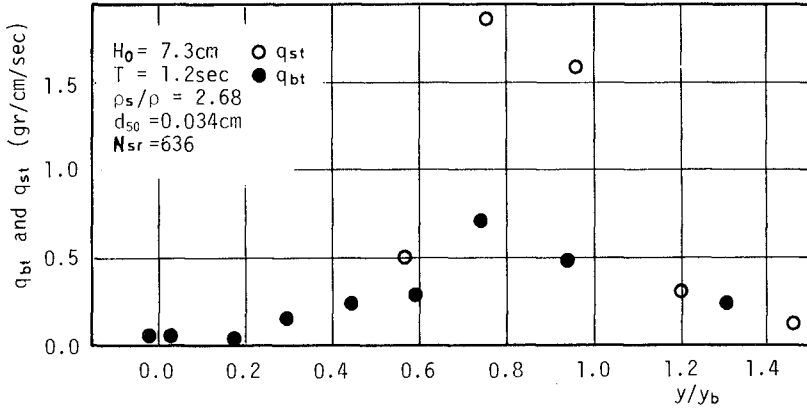


Fig.12(a) Distributions of  $q_{st}$  and  $q_{bt}$   
(  $N_{sr} = 636$  )

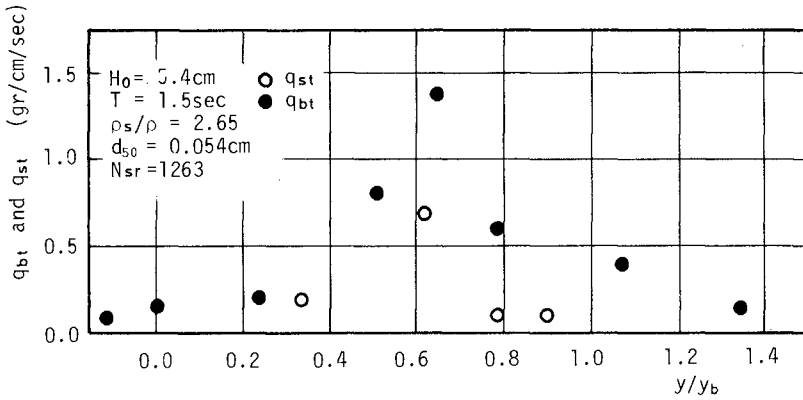


Fig.12(b) Distributions of  $q_{st}$  and  $q_{bt}$   
(  $N_{sr} = 1263$  )

Fig.13 shows one example of the distribution of  $q_{ynet}$ ,  $q_{bnet}$  and  $q_{snet}$  together with the beach profile of  $N_{sr}=636$ .  $q_{bnet}$  and  $q_{snet}$  were measured in a relatively short time compared with running time  $t_s/T=1.5 \times 10^3$ , in which the beach profile in Fig.13 was developed. So, they might change with running time.  $q_{ynet}$  is given as an average over  $t_s/T=0 \sim 1.5 \times 10^3$ . In Fig.13, the distribution of  $q_{bnet}$  is similar to that of  $q_{ynet}$ , and  $q_{snet}$  has a sharp peak at  $y/y_b=0.75$  which corresponds to the location of the bar. To examine the relative importance of  $q_{bnet}$  and  $q_{snet}$  in the beach deformation, the authors calculated the change of water depth caused by  $q_{bnet}$  and  $q_{snet}$  by using the equation of continuity of sediment transport without considering the effect of time-change of concentration of suspended sediment indicated by the first term in Eq.(15). The result is shown in Fig.14. In this figure,  $\Delta h$  shown by solid line is calculated from the difference of beach profiles between  $t_s/T=0$  and  $t_s/T=1.5 \times 10^3$ ,  $\Delta h_b$ , shown by heavy line, is calculated from  $q_{bnet}$  and represents the changes of mean water depth between two neighboring measuring points and  $\Delta h_s$ , shown by broken line is calculated from  $q_{snet}$  as well as  $\Delta h_b$ . As can be seen from this figure, the bar near  $y/y_b=0.75$ , the typical beach profile of this case, seems to be created not only by bed load but also by suspended load. However,  $\Delta h_s$  gives fairly large beach deformation compared with  $\Delta h$  in this region. According to Eq.(15), this difference between measured and calculated water depths have to be compensated by the increase of concentration of suspended sediment. On the other hand, the measured concentration increased about 6ppt at  $y/y_b=0.75$  during  $t_s/T=1.5 \times 10^3$ . This increment of concentration only accounts for few millimeter of erosion near  $y/y_b=0.75$ . This indicates that, even in the case where suspended load dominates bed load, the first term of Eq.(15) becomes less than 1/10 of other terms.

Fig.15 shows the relation between  $q_{ynet}$ ,  $q_{bnet}$  and  $q_{snet}$  in the case of  $N_{sr}=1263$ . In this case,  $q_{bnet}$  is in the direction of onshore through the entire range of the beach profile and the distribution of  $q_{bnet}$  almost coincides with  $q_{ynet}$ . While the direction of  $q_{snet}$  is mainly offshore and its magnitude is less than 1/2 of  $q_{bnet}$ . Fig.16 shows the relation between  $\Delta h$ ,  $\Delta h_b$  and  $\Delta h_s$ . Same notations and symbols as in Fig.14 are used. From this figure, it can be found that the fundamental mode of the beach deformation of Type III with deposition in the shallower region and erosion in the deeper region as shown in Fig.1 is mainly created by  $q_{bnet}$ . However,  $q_{snet}$  also seems to contribute to the beach deformation of secondary mode in addition to the fundamental mode.

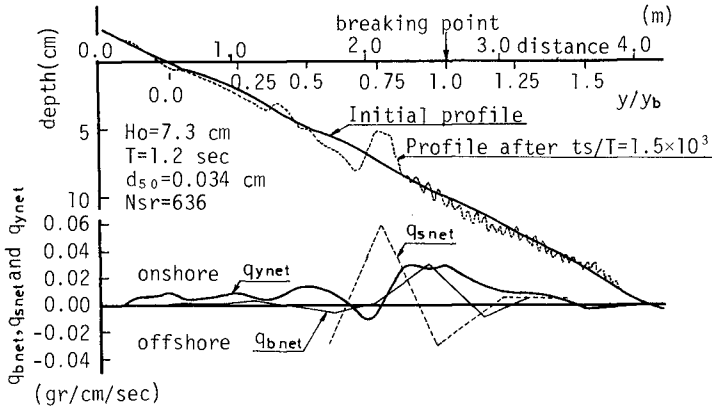


Fig.13 Beach profile and distributions of calculated and measured net on-offshore sediment transport rates (  $Nsr=636$  )

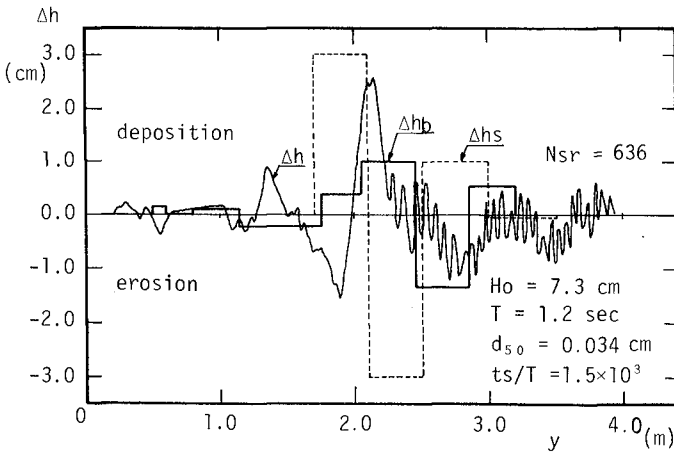


Fig.14 Comparison among  $\Delta h$ ,  $\Delta hb$  and  $\Delta hi$  (  $Nsr=636$  )

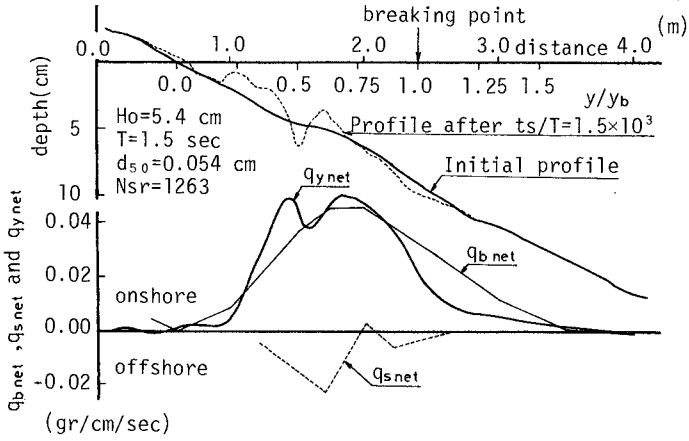


Fig.15 Beach profile and distributions of calculated and measured net on-offshore sediment transport rates (  $N_{sr}=1263$  )

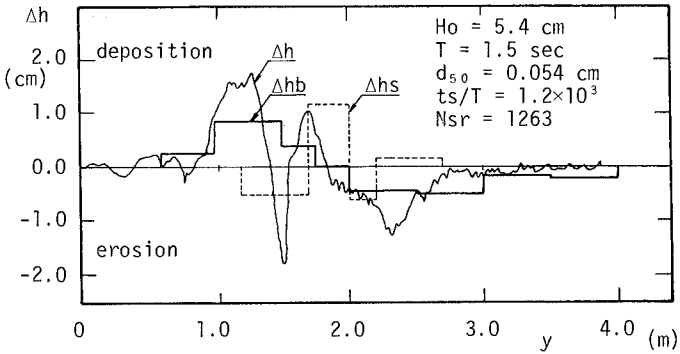


Fig.16 Comparison among  $\Delta h$ ,  $\Delta h_b$  and  $\Delta h_s$  (  $N_{sr}=1263$  )

### 5. Conclusions

The authors analyzed experimental results about the two-dimensional beach deformation conducted by many investigators to propose the models of net on-offshore sediment transport rate and carried out two-dimensional model beach experiments to examine the relative importance of bed load and suspended load in the beach deformation. Following results are obtained.

- 1) When  $N_{sr} = gT d_{50} / 2\pi v > 10^3$ , the direction of net sediment transport is onshore (Type III) and when  $N_{sr} < 10^3$ , net offshore sediment transport is apt to take place (Type I). However, even when  $N_{sr} < 10^3$ , net onshore sediment transport may spring up near the shore line.
- 2) Net onshore sediment transport decays faster than that of offshore sediment transport. And when  $N_s = H_o / T / \sqrt{(\rho_s / \rho - 1)} g d_{50}$  becomes large, net on-offshore sediment transport decays fast regardless of their direction.
- 3) The non-dimensional height of upper limit of beach deformation  $h_o / H_o$  increases with increasing  $\xi = i / \sqrt{H_o / L_o}$  and  $N_s$ . And the non-dimensional depth of lower limit of beach deformation  $h_m / L_o$  can be expressed by Eq.(6).
- 4) The maximum net offshore sediment transport takes place in the offshore region and the maximum onshore sediment transport takes place in the surf and swash zones. Time-variation of the maximum sediment transport rate can be approximated by Eq.(1). And its maximum can be expressed by Eqs.(12) and (13).
- 5) When  $N_{sr} > 1200$ , time-averaged bed load surpasses time-averaged suspended load, and main beach deformation seems to be created by bed load.
- 6) When  $N_{sr} < 640$ , time-averaged suspended load surpasses time-averaged bed load, and beach deformation seems to be caused by both bed load and suspended load.
- 7) Suspended load becomes equivalent in amount to bed load when  $u_* / w_o = 0.8$ .

### Acknowledgements

The authors gratefully acknowledge Dr. P.Eagleson, the former Associate Professor of Massachusetts Institute of Technology, Dr.B.Glenne the former Instructor of University of Colorado and Dr.J.Dracup, the former Assistant Professor of Oregon State College; Drs.M.Kurihara and K.Shinohara, the former Professors of Kyushu University, Dr.T.Tsubaki, the former Associate Professor of Yamaguchi University and Dr.M.Yoshidaka, the former Associate Professor of Miyazaki University; Dr.K.Horikawa, Professor of Tokyo University and Dr.T.Sunamura, the former Research Associate of Tokyo University; Dr.T.Izima and Mr.H.Aono, formerly Port and Harbour Technical Research Institute, Ministry of Transportation, Japan; Drs.R.Rector, T.Saville and G.Watts, formerly U.S.Army Beach Erosion Board; and Mrs.N.Tanaka and O.Shinbo, Port and Harbour Technical Research Institute, Ministry of Transportation, Japan for providing beach profiles for this report.

## References

- Battjes, J.A., Surf Similarity, Proc. 14th International Conf. Coastal Engg. pp 466-480, 1974.
- Bowen, A.J., Simple Models of Near Shore Sedimentation ; Beach Profiles and Longshore Bars, Proc. Coastaline of Canada Conf., in press, 1979.
- Dingler, J.R., Wave-formed Ripples in Near Shore Sands, Ph.d. Dissertation, Dept. of Oceanography, University of Carifornia, San Diego, 1975.
- Goda, Y., A Synthesis of Breaker Indices, Proc. of JSCE, No.180, pp 339-350, 1970. (in Japanese)
- Hallermeier, R.J., Calculating a Yearly Limit Depth to the Active Beach Profiles, CERC Ft. Belvoir, Va., Tech. Paper 77-9, 1977.
- Horikawa, K., T. Sunamura and H. Kondo, A Study of Beach Deformation by Wave Action, Proc. 21st Japanese Conf. Coastal Engg. pp 193-199, 1974. (in Japanese)
- Inman, D.L. and A.J. Bowen, Flume Experiment on Sand Transport by Waves and Currents, Proc. 8th International Conf. Coastal Engg. pp 137-150, 1963.
- Madsen, O.S. and W.D. Grant, Quantitative Description of Sand Transport by Waves, Proc. 15th International Conf. Coastal Engg. pp 1093-1112, 1976.
- Nakamura, M., H. Shiraishi and Y. Sakai, Wave Decaying due to Breaking, Proc. 10th International Conf. Coastal Engg. pp 234-253, 1966.
- Rector, R.L., Laboratory Study of Equilibrium Beach Profiles, BEB Washington D.C., TM-41, Aug. 1954.
- Sato, S. and N. Tanaka, Sand Movement due to Wave Action on a Horizontal bed, Proc. 9th Japanese Conf. Coastal Engg. pp 95-100, 1962. (in Japanese)
- Saville, T., Scale Effects in Two Dimensional Beach Study, Proc. 7th IAHR, pp A3-1 - A3-10, 1957.
- Sawaragi, T. and I. Deguchi, Distribution of Sand Transport rate Across a Surf Zone, Proc. 16th International Conf. Coastal Engg. pp 1596-1613, 1978.
- Swart, D.H., A Schematic of On-offshore Transport, Proc. 14th International Conf. Coastal Engg. pp 884-900, 1974.
- Tanaka, N. and O. Shinbo, The Properties of Coal Grains as Bed Material in the Model Beach Experiment on Littoral Drift, Report of the Port and Harbour Research Institute, Ministry of Transport, Vol.12, No.1, pp 3-58, March, 1973. (in Japanese)